IOP Publishing Journal of Physics D: Applied Physics
J. Phys. D: Appl. Phys. **00** (2015) 000000 (7pp) UNCORRECTED PROOF

A detailed Auger electron spectroscopy study of the first stages of the growth of C_{60} thin films

R A Vidal[1] **and J Ferrón**[1,2]

[1] Instituto de Física del Litoral (Universidad Nacional del Litoral—CONICET), Güemes 3450, (3000) Santa Fe, Argentina
[2] Departamento de Materiales, Facultad de Ingeniería Química, Universidad Nacional del Litoral, Santiago del Estero 2829, (3000) Santa Fe, Argentina

E-mail: julio.ferron@ifis.santafe-conicet.gov.ar

Received 22 May 2015, revised 7 August 2015
Accepted for publication 19 August 2015
Published

Abstract

In this work we take advantage of the large sensitivity and in-depth resolution of Auger electron spectroscopy (AES) to study in a detailed way the growth of C_{60} over different substrates, namely Cu(1 1 1), Si(1 0 0) and graphene. The ability of AES, as compared to more local probes like STM or AFM, to follow the process in a dynamic way, allows us to study the growth of C_{60} below and over one ML, including the change of C_{60} over either Si or Cu to the growth of C_{60} over a C_{60} film. We found that the growth proceeds always layer by layer. This result shows that differences in diffusion barriers are not as important as one may think following the idea of diffusion by a jumping mechanism. We propose that the sticking coefficient, governed by the adsorption energy, is responsible for the differences observed between Cu and Si. Our results also point to a different charge transfer among fullerene molecules and these surfaces. The same result is suggested in the case of C_{60} over graphene, but in this case our conclusion comes from the variable temperature experiments.

Keywords: C_{60}, copper, silicon, graphene film growth, surface diffusion, Auger electron spectroscopy, Monte Carlo method

AQ1 (Some figures may appear in colour only in the online journal)

1. Introduction

Since their discovery in the 1990s, [1] fullerenes have been extensively studied. Their applications cover an ample range of subjects, such as organic photovoltaic devices, chemistry, superconductors, single molecule transistors, etc [2]. Among the basic physical studies, the way C_{60} grows on different surfaces, including metals, semiconductors and insulators, is one of the most developed areas (see [3] and references therein). Due to its applications in optoelectronic and solar cell devices, the growth of C_{60} on Si is probably the most extensively studied system. But, even in this well known system some fundamental concepts are currently under discussion. For instance, a problem as basic as the charge transfer between the fullerene and the Si surface has still not been resolved. Thus, based on synchrotron photoemission spectroscopy, Moriarty *et al* [4] concluded that a chemical bond between C_{60} and both Si surfaces, i.e. Si(1 1 1) (7 × 7) and Si(1 0 0) (2 × 1) exists. On the other hand, using high resolution electron energy loss spectroscopy measurements (HREELS), Suto *et al* [5] determined that while a coverage dependent charge transfer occurs between the fullerene and the Si(1 1 1) surface, no charge transfer at all is detected on the Si(1 0 0) surface. To complete the picture: based on scanning tunneling spectroscopy (STS), Dunn *et al* [6] found a different charge transfer for different coverages not only for the Si(1 1 1) surface, as Suto *et al* did [5], but also for the Si(1 0 0) surface. Consequently, it appears quite evident that the full picture of the growth of C_{60} on Si surfaces is not fully understood yet.

JNL:JPD PIPS: AA0237 TYPE: PAP TS: NEWGEN DATE:7/9/15 EDITOR: IOP SPELLING: US

What happens with the growth of C_{60} on other surfaces like metallic ones? The state of the art here is similar to the semiconductor case. Thus, a net charge transfer of one electron per C_{60} cage from the Cu(1 1 1) substrate was determined using STM, and theoretically predicted by a model based on a local density approximation [7]. However 1.5 to 2 electrons per C_{60} molecule was found, for the same system, using photoelectron spectroscopy (PES) and near-edge-x-ray absorption spectroscopy (NEXAFS) [8]. On the other hand, Sakurai *et al* [9] determined crucial differences between C_{60} growing on Cu(1 1 1) and Ag(1 1 1). They found that while on Cu(1 1 1) the strong interactions between C_{60} molecules and the substrate prevail, on Ag(1 1 1) the interactions between C_{60} molecules are dominant. It is known that C_{60} starts decorating the step-edges on Cu(1 1 1), with the appearance of 2D islands only after the completion of this stage [7]. Upon annealing, above 500 K, a well ordered close-packed monolayer showing a (4×4) LEED pattern [7] is formed. Recently, STM studies showed that Cu(1 1 1) surfaces reconstruct under a C_{60} monolayer [10]. To add experimental data to the discussion, a charge transfer of three electrons per C_{60} molecule from the Cu surface is determined by angle resolved photoelectron spectroscopy (ARPES) [11]. The origin of this large charge transfer was linked to a (4×4) reconstructed interface with seven Cu atom vacancies in the interface [11]. These results have been supported recently by a detailed LEED analysis [12]. The picture is then quite similar to the C_{60}/semiconductor system, i.e. we have a lot of experimental results but, at the same time, we have a lot of questions.

An alternative substrate on which to grow C_{60} molecules is highly oriented pyrolytic graphite (HOPG). It is known that the C_{60} interaction with the HOPG surface is weak, and no charge transfer from or to the fullerene molecule has been observed by Liu *et al* [13]. They also showed that the growth of the first layer is completely different from the growth of the second and subsequent layers. Thus, while the first layer grows in round and elongated islands the second layer is characterized by fractal-dendritic shaped islands. The authors suggested that the very different growth modes arise from the significant differences in the diffusion energies of C_{60} on HOPG and on a C_{60} film. In fact, while the C_{60}-HOPG interaction is about 20% stronger than the C_{60}–C_{60}(1 1 1) interaction (968 and 813 meV, respectively) the diffusion barrier is an order of magnitude smaller (13 and 168 meV, respectively) [14]. In a later paper Liu *et al* [15] presented kinetic Monte Carlo simulations to understand the fractal-dendritic growth of C_{60} islands on compact first layer islands on HOPG at the molecular level.

In this work we study the growth of C_{60} on semiconductor (Si); metal (Cu) and graphene supported on Cu. The growth of C_{60} over different substrates represents an interesting model for surface diffusion studies. The parameters governing the growth of films are: (i) *the diffusion barrier* is the energy needed by a molecule to move to a near site; (ii) *the Ehrlich–Schwoebel barrier* is the extra energy needed by molecules in order to be able to diffuse over a step to the down terrace; (iii) *the sticking coefficient* is the probability of a molecule ~~attaching~~ to the surface, ~~it is~~ related to the binding energy. We can always play on any system with substrate temperatures and flux rates in order to change the growing conditions, but working with C_{60} allows us to strongly change all these parameters by just going from the first to the second layer, i.e. keeping substrate temperature and molecule flux constants. Our intention is to use this change to gain knowledge about the surface diffusion mechanisms. While the growth of fullerenes over different surfaces depends on C_{60}–surface interactions, the growth of the second layer will depend on the way the first layer is formed. Recently, Amelines-Sarria *et al* [2] investigated the growth morphology, as well as other electronic and magnetic properties, of C_{60} thin films ($\geqslant$4 ML) grown on different substrates. They found that films exhibit nanometric aggregates whose size increases with film thickness, irrespective of the substrate. Thus, their results support that the C_{60} film determines the growing conditions. In this paper we study different growth regimes, showing that at the first stages, the role of the substrate is relevant. We use Auger electron spectroscopy (AES) to characterize the first stages of growth. AES has been used to study the growth of C_{60} over different substrates in a very limited way. The reason is that the spatial (2D) resolutions of STM, and the chemical one of XPS, are unbeatable. However, the in-depth resolution and sensitivity of AES, mainly when using low energy electrons, are undoubtedly superior to those of XPS allowing us to follow the growth in greater detail. We complete our study with simple simulations based on a kinetic Monte Carlo (kMC) model. The goal of this part of the work is to help us understand the changes on the growth kinetic.

2. Experimental methods

The AES experiments were performed in a commercial surface analysis system (PHI SAM 590A) with a base pressure in the low 10^{-10} Torr. Fullerene films were deposited by sublimation of C_{60} from a Knudsen cell onto Si(1 0 0), Cu(1 1 1) and a commercial graphene grown on polycrystalline copper [16] substrates. The cell was carefully degassed and shuttered to avoid sample contamination. The Si(1 0 0) [Cu(1 1 1)] single crystal was cleaned by cycles of ion bombardment and annealing using Ar^+ ions of 1 keV [2 keV] and annealing temperatures of 1200 K [800 K] for 2 min [5 min] until no sign of contamination was detectable in the AES spectra. Samples of graphene grown on copper foil by CVD could be heated up to 1070 K without desorption [16]. The samples were heated by electron rear bombardment and the temperature measured by a chromel – alumel thermocouple. Auger spectra were acquired using a cylindrical mirror analyzer in the differentiated mode (with 4 V_{p-p} modulation amplitude), a primary electron energy of 3 keV and an analyzer resolution of 0.3%. The electron beam current was fixed at 1 μA (current density ~ 1 mA cm^{-2}). During the growth of a C_{60} film Auger spectra were acquired in an alternating fashion.

The quality of C_{60} films was checked, in addition to AES, by means of electron energy loss spectroscopy (EELS) using the same setup (100 eV primary electrons, 0.3% resolution). The 5.9 eV characteristic π plasmon of C_{60} (and HOPG) was used as a signature of the C_{60} film growth. In figure 1 we

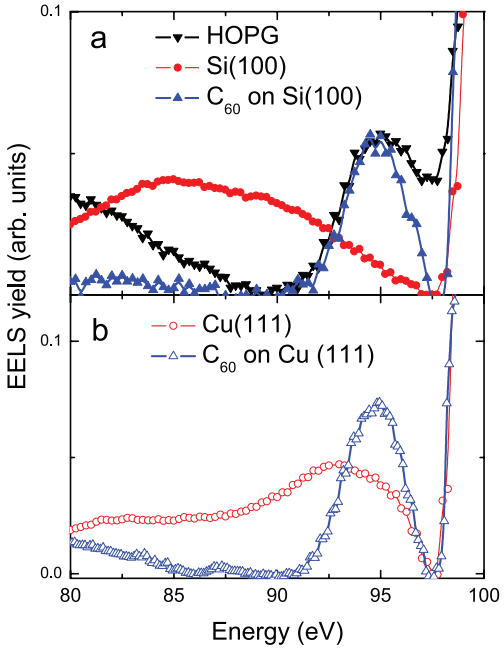

Figure 1. (a) EELS for HOPG, Si(1 0 0) and C_{60} on Si(1 0 0), (b) EELS for Cu(1 1 1) and C_{60} on Cu(1 1 1). EELS acquired with 100 eV primary electrons. C_{60} films are multilayer (more than 3 ML).

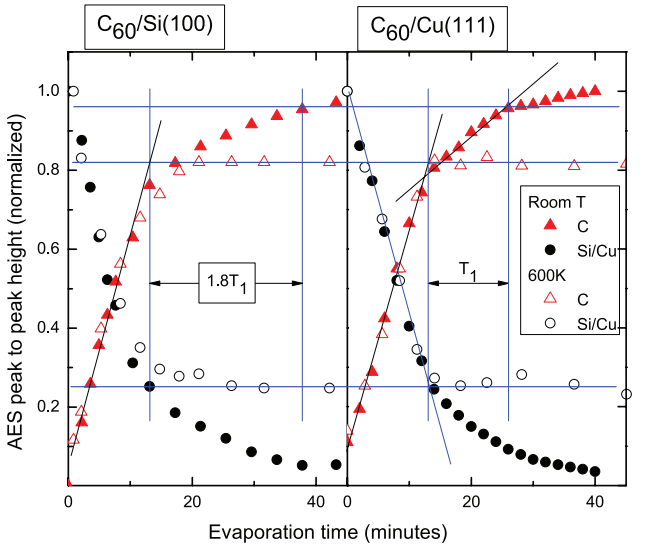

Figure 2. AES peak-to-peak evolution of C_{KLL} and Si_{LVV} (Cu_{MVV}) during C_{60} evaporation. Left on Si(1 0 0), right on Cu(1 1 1). Full symbols RT, open ones 600 K. Substrate signals (Si_{LVV}, Cu_{MVV}) have been normalized to the clean substrate signal, while C_{60} signal (C_{KLL}) has been normalized to a thick C_{60} film signal. Horizontal lines correspond to the expected values for the first and second C_{60} layers, see text.

depict the π plasmon signature for C_{60} on Cu and Si. Si and Cu plasmon peaks are clearly shown for the clean substrate prior to the film growth. The HOPG energy loss spectrum is also shown for comparison.

3. Results and discussions

Figure 2 left (right) shows AES peak-to-peak heights for the Si $_{LVV}$ and C $_{KLL}$ (Cu_{MNN} and C_{KLL}) Auger transitions while sublimating C_{60} molecules on Si(1 0 0) (Cu(1 1 1)) at RT and 600 K. Although some of the results depicted in these figures were already known [17], these curves give us an important amount of information. The growth process is governed by two key parameters: the diffusion barrier and the adsorption energy. The beauty of the systems studied in this work is that both parameters change dramatically once the first monolayer is completed. For example, as we mentioned in the introduction, the diffusion barrier changes from 13 meV for C_{60} on HOPG to 160 meV for C_{60} on C_{60}.

The Auger time profile, as we pointed out above, lets us follow the changes in adsorption conditions during growth in a unique way. Let us see first the Auger evolution of both systems at room temperature (RT). Layer by layer (LbL) growth is characterized in AES by straight lines of different slopes between breaks, pointing out each break a layer completion [18]. The closer the growth is to a perfect LbL, the better the breaks and the slopes are defined. Within this context, the growth of C_{60} on Cu appears, in our results, smoother than on Si. For C_{60}/Cu we can identify, in the C Auger evolution, even the second break corresponding to the completion of the second layer.

The experiments on Cu give us at least two startling results. The first is the LbL growth beyond the second layer. This is an unexpected result taking into account the large differences between both surface diffusion barriers, i.e. C_{60} on Cu surface versus C_{60} on C_{60} monolayer. Another surprising result is that it takes roughly the same time to grow the first and second layers of C_{60} (time needed to grow the first C_{60} layer, $T_1 = 13$ min within our experimental conditions). Due to the different adsorption energies that give, supposedly, different sticking coefficients, one would expect that the time needed to grow C_{60} over the C_{60} first layer should be larger than that over clean Cu. This is just what occurs for the Si substrate. Here, the completion of the second layer nearly duplicates the time needed to grow the first one ($1.8T_1$). This result points to different sticking conditions for C_{60} on Si with respect to C_{60} on C_{60} films. As a summary of this section we have more questions than answers. C_{60} grows in a rather similar way over Cu and over a C_{60}/Cu film, but it shows more difficulties in growing over Si and also over C_{60}/Si. These results cast doubt not only on the charge transfer between fullerenes and Si and Cu, but also on the surface diffusion mechanism. Taking into account the almost perfect LbL growth of C_{60} over both Cu and the fullerene film, perhaps an atomic/molecular interchange diffusion model [19] should not be discarded instead of the commonly assumed jumping one.

However, the growth of C_{60} on metals and semiconductors is dramatically different from its behavior on a C_{60} film. In figure 2 we show the adsorption process over a heated substrate. With the sample at 600 K we are not able to grow more than one (the first) monolayer over both substrates. While the growth of C_{60} over a metal or a semiconductor suffers only minimal changes at 600 K (mostly on Si close to the

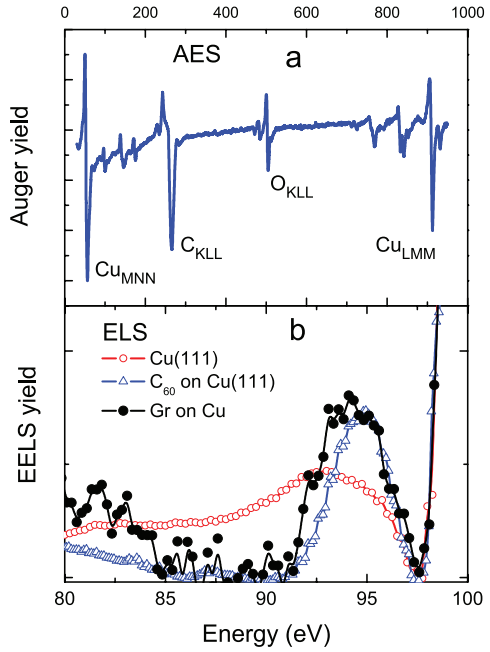

Figure 3. AES (a) and EELS (b) yields for graphene on Cu. The plasmon peaks of Cu(1 1 1) and C_{60} on Cu(1 1 1) are kept for comparison.

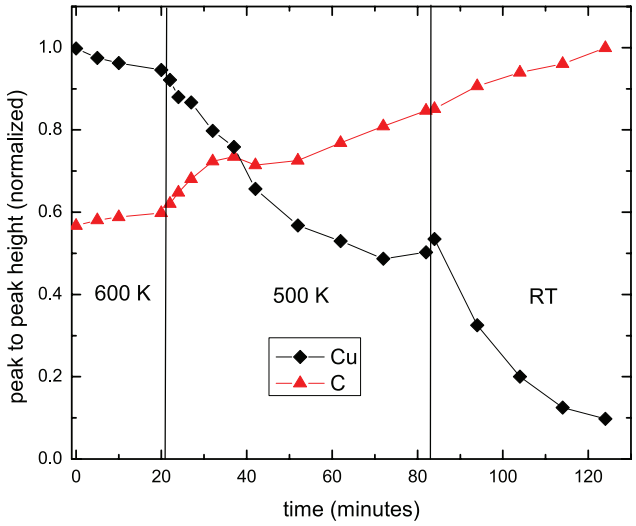

Figure 4. AES peak-to-peak evolution of C_{KLL} and Cu_{MVV} during C_{60} evaporation over a graphene/Cu layer. The growth is performed at different substrate temperatures, as shown in the figure. Cu_{MVV} signal has been normalized to the clean substrate signal, while C_{60} signal (C_{KLL}) has been normalized to a thick C_{60} film signal.

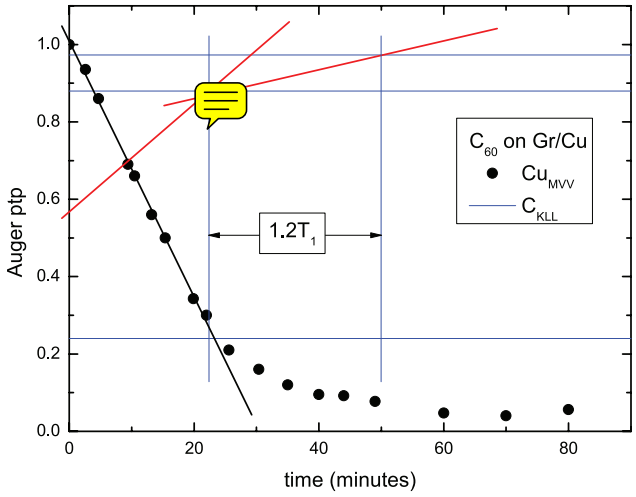

Figure 5. AES peak-to-peak evolution of C_{KLL} and Cu_{MVV} during C_{60} evaporation over a graphene/Cu layer. The growth is performed at room temperature.

completion of one ML), the sticking coefficient of C_{60} over a C_{60} film falls down to zero.

As we said in the introduction, there are techniques with better chemical (XPS) and topographical (STM) resolution than AES, however, none of these allow us to follow the growth in such a detailed way as the results depicted in figure 2. Even though the linear dependence and the breaks are enough evidence of an LbL growth, we have another quantitative evidence supporting the LbL interpretation of the experiments depicted in figure 2. For instance, it seems quite reasonable to assume that the saturation of the C_{KLL} Auger yield evolution at 600 K corresponds to the completion of the first layer. The Auger yield dependence for a growing film is of the type $(1 - e^{-x/(\lambda<\cos(\theta)>)})$, where λ is the Auger escape depth and $<\cos(\theta)>$ is the average cosine of the electron emission angle with respect to surface normal (for $\theta = 30°$,$<\cos(\theta)>$ =0.63). With the experimental yield of 0.82 and assuming a reasonable value of 1 nm for λ [20], we obtain 1 nm for the C_{60} film thickness, in good agreement with reported C_{60} cage diameters [21]. With this value for the first layer, we can estimate the expected value for the second layer, and for the same experimental condition. This calculation gives a C_{KLL} Auger yield of 0.96, in a nice agreement with the idea that the second break corresponds to the completion of the second layer. The conclusion of this part of the experiment is then encouraging: (i) C_{60} grows LbL on Si(1 0 0), at least until the first layer completion, and on Cu(1 1 1) up to the Auger detection limit; (ii) the high temperature experiments show the different adsorption energies among C_{60} on a C_{60} film, on metallic and semiconductor surfaces.

So far we have reasonably characterized the growth of C_{60} on a metal (Cu) and on a semiconductor (Si). To have a more complete picture of the growth mechanisms, it would be interesting now to study the growth of C_{60} on a semimetal. Although the system C_{60}/HOPG is a good candidate, and as such has been extensively studied [2, 13, 15, 22], it is clear that being carbon over carbon AES is useless. Although there are differences in the C_{KLL} Auger line shape among amorphous C, C_{60}, diamond, graphene and HOPG [23], it would be an impossible task to differentiate them during a growing process where a mixture of these signals might coexist. Thus, all C_{60}/HOPG studies have been performed with topographical tools like AFM and STM. To solve this problem, we used graphene grown on Cu as substrate [16]. In figure 3(a) we show the Auger spectrum of this commercial graphene layer. The copper used for this purpose presents some degree of contamination, oxygen and minor amounts of P and S, but the graphene electronic features appear reasonably well, as they are represented by the π plasmon peak (figure 3(b)), and the

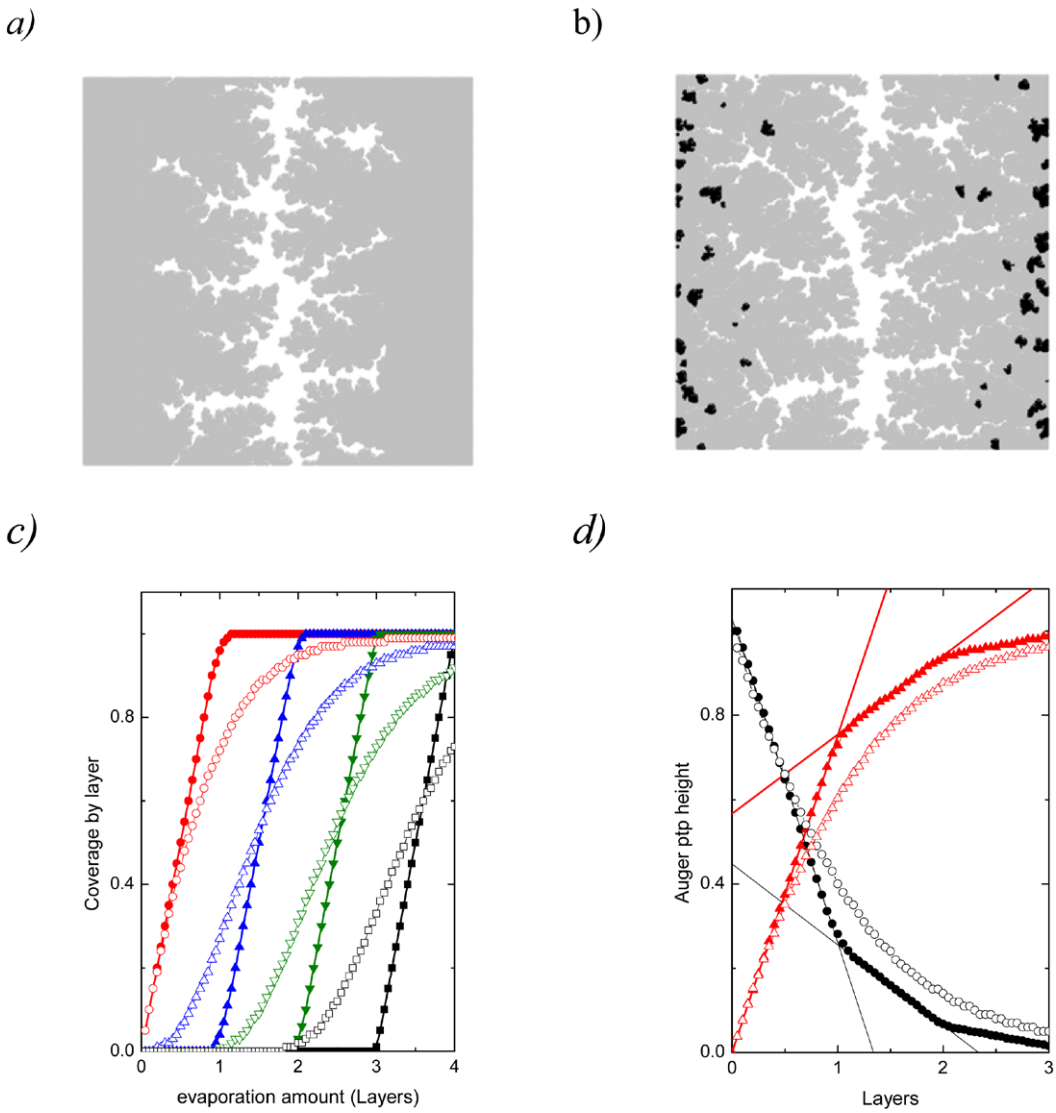

Figure 6. ~~Left:~~ coverage evolution for different growth modes; (a) and (b), snapshots of KMC growth for 0.8 ML and different diffusion lengths. In (c) we depict the coverage evolution and in (d) the Auger ptp yields. Full symbols correspond to an LbL growth ($N = \infty$), and empty symbols to a limited diffusion length leading to a 3D growth. (a) $\lambda_{1st\ Lay} \sim \infty \sim \lambda_{2nd\ Lay}$, (b) $\lambda_{1st} \sim \infty$; $\lambda_{2nd\ Lay} \sim 20\%$ of terrace size.

Raman spectrum provided by the suppliers (not shown in this work). The plasmon peak appears slightly wider than for C_{60}, due to the contribution of the substrate, i.e. the graphene layer is thinner than the C_{60} film. On the other hand, the knowledge of the initial ratio between the C_{KLL} and Cu_{MVV} Auger yields allows us to follow the film growing process by AES.

In figure 4 we show the growth of C_{60} on a graphene/Cu surface for different substrate temperatures, in a similar way as the experiments for Si and Cu depicted in figure 2. The results are different for this last substrate from the very beginning, thus almost no C_{60} nucleates over the surface at 600 K. This result can be easily understood, i.e. the binding energy of fullerenes is lower on graphene than on either Cu or Si. If we lower the substrate temperature, down to 500 K first and RT later, the growth of the first and subsequent layers is then possible. As expected, the growth rate increases for lower temperatures as a consequence of the increase of the sticking probability.

In order to gain insight about the growth mechanism of C_{60} over graphene, we need to perform the full process at room temperature. In figure 5 we show the results corresponding to this experiment. They point again to an LbL growth with a quite similar behavior for the first and second layers.

The almost perfect LbL growth of C_{60} beyond the first layer over all these substrates is a rather surprising result. It points to the weak influence of the different C_{60} molecule diffusion barrier heights over the different substrates. In fact, there is a consensus that C_{60} should diffuse better over a less corrugated surface like Cu, Si and graphene, than over a C_{60} film. This assumption appears, at first sight, to disagree with our experimental results. However, we must keep in mind that this kind of diffusion barrier assumes a jumping based mechanism. If an atomic or molecular exchange mechanism is likely we can look at the process from a different point of view. In this way, our experimental results do not contradict previous findings, i.e. the growth of the second layer may be either fractal, as

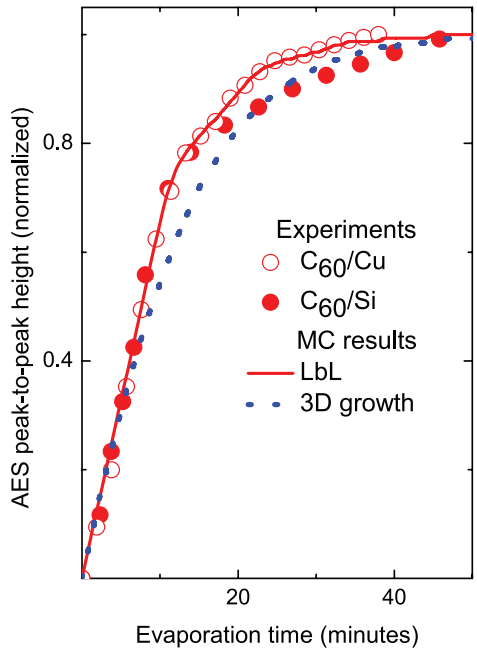

Figure 7. Auger evolution of the growth of C_{60} (symbols) compared to MC simulations (lines).

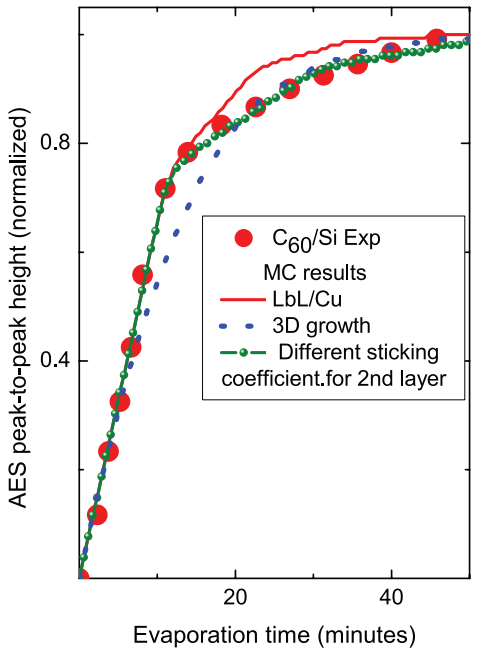

Figure 8. Auger evolution of the growth of C_{60} on Si (symbols) compared to MC simulations corresponding to LbL, 3D and with a lower sticking coefficient for the second layer.

compared to the more rounded islands obtained for the first layer by Liu and Reinke [13], or fractal from the very beginning as suggested by the group of Kappes [21] but in any case our results show that the first layer is complete before the second layer starts to grow.

It is clear that the growth of C_{60} over the different surfaces studied so far presents several similarities, but there are also some differences. The growth over Si(1 0 0) is the 'worst' to be characterized as LbL. Although the quantitative results point in that direction, i.e. the saturation value obtained at 600 K is quite the same as where the first break appears, it is however clear that this break is less pronounced than in the other two cases. The imperfection in the growth, as detected by AES, in the Si case could be explained either as a departure from the LbL growth, where the larger C_{60}/C_{60} diffusion barrier would be responsible, or as a delay of the LbL growth due to different sticking coefficients. In order to answer this question we performed a simple simulation based on kinetic MC ideas.

The idea behind the MC simulation is not to determine the growing process mechanisms. To do that we should use MC approaches based on realistic potentials, like those we used to study the growth of Cu and Co on Cu(1 1 1) [24]. In this work we only intended to model the different AES peak-to-peak evolutions arising from the different possible ways of growing. We used the simple DLA (diffusion-limited aggregation) model [25]. Within this model, we have a perfect surface with periodic conditions, and one (or more) nucleation centers or a step-edge. A molecule is deposited over the surface and allowed to move with no restriction. The molecule moves until:

(i) it encounters a nucleation center, where it nucleates;
(ii) it executes a determined number of jumps (N).

The number of allowed jumps (N) is just the key parameter that determines the way of growth. The probability of a molecule either finding a nucleation center, or jumping to a lower terrace, to allow the LbL growth, and becoming a new possible nucleation center is proportional to N. N is related to the diffusion length and it is physically determined by the surface temperature and diffusion barriers.

In figures 6(a) and (b), we show two snapshots obtained from the KMC growth simulation. The first corresponds to an LbL growth. The terrace is limited by two nucleating steps and the molecules have enough time to reach each step and nucleate there. Since the diffusion length on the second layer is also infinite, molecules also have enough time to descend to the lower terrace. We should note that in this simulation no Ehrlich–Schwoebel [26] barrier is considered, i.e. molecules can freely descend to the lower terrace. In figure 6(b) we consider a layer diffusion length lower than the terrace size (20% of it). This new scenario opens the possibility of the molecules nucleating over the second layer. This particular simulation resembles a system with different diffusion barriers like those we expect when changing from the growth of C_{60} on Cu to the growth of C_{60} on C_{60}. In the second row of figures 6(c) and (d) we show the evolutions of coverage and Auger peak-to-peak heights for the same growing conditions of the snapshots.

The coverage evolution clearly shows, for the LbL growth (full symbols in figure 6(a)), the completion of each layer before the next layer starts to grow. When the diffusion path of the second layer is reduced (open symbols in figure 6(c)), the second, and even third layer coverage starts before the completion of the first. In the same way, the Auger evolution shows clear breaks and a linear behavior between them in the case of Lbl growth, and the loss of these conditions in the 3D growth case (full and open symbols in figure 6(d)).

Let us now apply these results to analyze the experimental results for the growth of C_{60} over Cu and Si. Since in this

kind of MC simulation the time is not a known variable, we can use some experimental data to correlate time to jumps. Thus, we fit the LbL part of the growth (growth for low coverages), using then the same parameters for larger coverages. In figure 7 we show results obtained through this procedure compared to the experimental results.

As we expected, the LbL growth evolution obtained with the MC simulation agrees nicely with the experimental results for the growth of C_{60} over Cu (continuous line), but the simulation starts to deviate for the Si substrate beyond the completion of the first layer. The limitation of the diffusivity on the second layer, with the 3D growth incorporation (dotted line), is not a solution to this experimental behavior. In fact, the Auger behavior is more sensitive to the development of the second layer than to the subsequent ones, thus we cannot fit both parts of the experiment: the simulated AES ptp falls down the experiment before the completion of the first layer, and gives larger values as the film grows beyond the second.

In order to understand the behavior of the C_{60} over Si system we analyzed the second possibility, i.e. a change in the sticking coefficient. In figure 8, we depict the MC results considering the effect of lowering the sticking coefficient for the second layer, i.e. C_{60} over C_{60}, to a 60% of its value on Si. With only this assumption we can fit the experimental results nicely. In the figure we repeat, in order to facilitate the comparisons, the experimental results for C_{60} over Si and the MC results for LbL and 3D growth, already shown in figure 7. The agreement of this simulation with the experiments is clear. Thus, we can explain all our experimental results about the growth of C_{60} on metal and semiconductor as an LbL mode with only the assumption of a lower sticking coefficient in the case of the Si substrate. One important physical fact behind this behavior is that it suggests a different charge transfer between the C_{60} molecule and both substrates, i.e. Si and Cu.

AQ2

4. Conclusions

The advantage of using Auger electron spectroscopy instead of more local probes (e.g. STM) is its ability to dynamically follow the growth process. Using AES to study the growth of C_{60} over Cu(1 1 1), Si(1 0 0) and graphene on copper, we find that, in spite of the proved differences among the fullerene diffusion barriers on each of these surfaces (including a C_{60} ML), the growth proceeds always in a layer by layer fashion. This fact means that the diffusion barrier is not the key physical parameter ruling this process. On the other hand, the sticking coefficient, governed by the adsorption energy, appears to be responsible for the differences observed between Cu and Si. This result points to a different charge transfer between the fullerene molecule and these surfaces. On the other hand, we found that C_{60} behaves on graphene in a rather similar way as it does on C_{60}, pointing again to the adsorption energy as the key parameter.

AQ3

Acknowledgments

We gratefully acknowledge Dr S Montoro and Dr N Bajales for their help in the laboratory. This work was financially supported by CONICET, ANPCyT and UNL, through projects PIP 2012–2014, grant no. 577; PICT 2010, grant no. 0294 and PICT 2013, grant no. 0164; and CAI + D 2011, grant no. 501 201101 00283 LI (A); respectively.

AQ4

References

[1] Kroto H W, Heath J R, O'Brien S C, Curl R F and Smalley R E 1985 *Nature* **318** 162
[2] Amelines-Sarria O *et al* 2011 *Org. Electron.* **12** 1483
[3] Moriarty P J 2010 *Surf. Sci. Rep.* **65** 175
[4] Moriarty P J, Upward D, Dunn A W, Ma Y, Beton P H and Teehan D 1998 *Phys. Rev.* B **57** 362
[5] Suto S, Sakamoto K, Chang-Wu Hu T and Kasuya A 1997 *Phys. Rev.* B **56** 7439
[6] Dunn A W, Svensson E D and Dekker C 2002 *Surf. Sci.* **498** 237
[7] Hashizume T *et al* 1993 *Phys. Rev. Lett.* **7** 2959
[8] Tsuei K-D, Yuh J-Y, Tzeng C, Tchu R-Y, Chung S-C and Tsang K-L 1997 *Phys. Rev.* B **56** 15412
[9] Sakurai T, Wang X, Hashizume T, Yurov V, Shinohara H and Pickering H W 1995 *Appl. Surf. Sci.* **87** 405
[10] Pai W W, Ching-Ling H, Lin M C, Lin K C and Tang T B 2004 *Phys. Rev.* B **69** 125405
[11] Pai W W *et al* 2010 *Phys. Rev. Lett.* **104** 036103
[12] Xu G, Shi X Q, Zhang R Q, Pai W W, Jeng H T and Van Hove M A 2012 *Phys. Rev.* B **86** 075419
[13] Liu H and Reinke P 2006 *J. Chem. Phys.* **124** 164707
[14] Gravil P A, Devel M, Lambin Ph, Bouju X, Girard Ch and Lucas A A 1996 *Phys. Rev.* B **53** 1622
[15] Liu H, Lin Z, Zhigilei L V and Reinke P 2008 *J. Phys. Chem.* C **112** 4687
[16] Graphene Supermarket Graphene Laboratories Inc. https://graphene-supermarket.com/
[17] Dutton G and Zhu X 2002 *J. Phys. Chem.* B **106** 5975
[18] Argile C and Rhead G E 1989 *Surf. Sci. Rep.* **10** 277
[19] Feibelman P J 1990 *Phys. Rev. Lett.* **65** 729
[20] Powell C J NIST Electron Inelastic-mean-free-path database, NIST Standard Reference Database 71, V1.1
[21] Dresselhaus M S, Dresselhaus G and Eklund P C 1996 *Science of Fullerenes and Carbon Nanotubes* (New York: Academic)
[22] Jester S, Löffler D, Weis P, Böttcher A and Kappes M M 2009 *Surf. Sci.* **603** 1863
[23] Pregliasco R G, Zampieri G, Huck H, Halac E B, de Benyacar M A R and Righini R 1996 *Appl. Surf. Sci.* **103** 261
Hamza A V and Balooch M 1993 *Chem. Phys. Lett.* **201** 404
Galuska A A, Madden H H and Allred R E 1988 *Appl. Surf. Sci.* **32** 253
[24] Gómez L, Slutzky C, Ferrón J, de la Figuera J, Camarero J, Vázquez de Parga A L, de Miguel J J and Miranda R 2000 *Phys. Rev. Lett.* **84** 4397
Camarero J, Ferrón J, Cros V, Gómez L, Vázquez de Parga A L, Gallego A M, Prieto J E, de Miguel J J and Miranda R 1998 *Phys. Rev. Lett.* **81** 850
[25] Witten T A Jr and Sander L M 1981 *Phys. Rev. Lett.* **47** 1400
Meakin P 1983 *Phys. Rev.* A **27** 1495
[26] Ehrlich G and Hudda F G 1966 *J. Chem. Phys.* **44** 1039
Schwoebel R J and Shipsey E J 1966 *J. Appl. Phys.* **37** 3682

QUERIES

Page 1
AQ1
Please be aware that the colour figures in this article will only appear in colour in the online version. If you require colour in the printed journal and have not previously arranged it, please contact the Production Editor now.
Page 7
AQ2
Section headings have been ordered sequentially as per the journal style. Please check and approve.
AQ3
We have been provided funding information for this article as below. Please confirm whether this information is correct.
FONCYT: PICT-2013-0164.
AQ4
Please check the details for any journal references that do not have a link as they may contain some incorrect information.
AQ5
Please update the year of publication and publication details for references [16, 20].